CD36 Is a Matrix Metalloproteinase-9 Substrate that Stimulates Neutrophil Apoptosis and Removal during Cardiac Remodeling

Kristine Y. DeLeon-Pennell, PhD[1], **Yuan Tian, PhD**[1], **Bai Zhang, PhD**[2], **Courtney A. Cates, MS**[1], **Rugmani Padmanabhan Iyer, PhD**[1], **Presley Cannon, MS**[1], **Punit Shah, PhD**[2], **Paul Aiyetan, MS, MD**[2], **Ganesh V. Halade, PhD**[3], **Yonggang Ma, PhD**[1], **Elizabeth Flynn, BS**[1], **Zhen Zhang, PhD**[2], **Yu-Fang Jin, PhD**[1,4], **Hui Zhang, MS, PhD**[2], and **Merry L. Lindsey, PhD**[1,5]

[1]Mississippi Center for Heart Research & San Antonio Cardiovascular Proteomics Center, Department of Physiology & Biophysics, University of Mississippi Medical Center, Jackson, MS

[2]Department of Pathology, Johns Hopkins University School of Medicine, Baltimore, MD

[3]Division of Cardiovascular Disease, The University of Alabama at Birmingham, Birmingham, AL

[4]Department of Electrical & Computer Engineering, The University of Texas at San Antonio, San Antonio, TX

[5]Research Service, G.V. (Sonny) Montgomery Veterans Affairs Medical Center, Jackson, MS

Abstract

Background—After myocardial infarction (MI), the left ventricle (LV) undergoes a wound healing response that includes the robust infiltration of neutrophils and macrophages to facilitate removal of dead myocytes as well as turnover of the extracellular matrix (ECM). Matrix metalloproteinase (MMP)-9 is a key enzyme that regulates post-MI LV remodeling.

Methods and Results—Infarct regions from wild type and MMP-9 null mice (n=8/group) analyzed by glycoproteomics showed that of 541 *N*-glycosylated proteins quantified, 45 proteins were at least two-fold up- or down-regulated with MMP-9 deletion (all p<0.05). Cartilage intermediate layer protein (CILP) and platelet glycoprotein 4 (CD36) were identified as having the highest fold increase in MMP-9 null mice. By immunoblotting, CD36 but not CILP decreased steadily over the time course post-MI, which identified CD36 as a candidate MMP-9 substrate. MMP-9 was confirmed *in vitro* and *in vivo* to proteolytically degrade CD36. *In vitro* stimulation of day 7 post-MI macrophages with MMP-9 or a CD36 blocking peptide reduced phagocytic capacity. Dual immunofluorescence revealed concomitant accumulation of apoptotic neutrophils in the MMP-9 null group compared to WT. *In vitro* stimulation of isolated neutrophils with MMP-9 decreased neutrophil apoptosis, indicated by reduced caspase-9 expression.

Correspondence: Kristine Y. DeLeon-Pennell, PhD, Department of Physiology and Biophysics, University of Mississippi Medical Center, 2500 North State St., Jackson, MS 39216-4505, Tel: 601-815-0816, Fax: 601-984-1817, kdeleon@umc.edu. Merry L. Lindsey, PhD, Department of Physiology and Biophysics, University of Mississippi Medical Center, 2500 North State St., Jackson, MS 39216-4505, Tel: 601-815-1329, Fax: 601-984-1817, mllindsey@umc.edu.

Conclusions—Our data reveals a new cell signaling role for MMP-9 through CD36 degradation to regulate macrophage phagocytosis and neutrophil apoptosis.

Keywords

extracellular matrix; proteomics; metalloproteinase; myocardial infarction; platelet glycoprotein 4

Introduction

Myocardial infarction (MI) is a significant contributor to the high morbidity and mortality rates associated with cardiovascular disease.[1] Following MI, the left ventricle (LV) undergoes a wound healing response comprised of robust infiltration of inflammatory cells that regulate extracellular matrix (ECM) turnover to remove necrotic debris and form an infarct scar.[2] In the mouse model of MI, the inflammatory response begins to subside by day 7, leading the way for an increase in ECM production and scar formation.

Matrix metalloproteinases (MMPs) are zinc-dependent enzymes that proteolytically process ECM proteins, cytokines, chemokines, growth factors, and adhesion molecules.[3, 4] MMP cleavage can activate or inactivate a protein; for example, cleavage of interleukin (IL)-8 increases its activity while cleavage of Cxcl4 decreases its activity.[5] MMP-9 is particularly important in the post-MI setting, as protein concentrations increase 3-fold in the infarct region during the first week post-MI.[6, 7] MMP-9 deletion attenuates LV dilation post-MI, indicating a causal role for MMP-9.[6, 8] Although a number of *in vitro* MMP-9 substrates have been identified, including collagens (IV, V, VII, X and XIV), gelatin, fibronectin, elastin, IL-8, Cxcl4, and IL-1β, the mechanisms whereby MMP-9 modulates post-MI LV remodeling has not been completely elucidated.[9, 10]

Methods

Detailed methods are described in the Supplemental Methods.

Mice

C57BL/6J wild type (WT) and MMP-9 null male and female mice of 4–7 months of age were used in this study (Supplemental Table S1). The MMP-9 null mice were generated by Zena Werb's laboratory and backcrossed onto the C57BL/6J strain by Lynn Matrisian's laboratory.[11, 12] Mice were kept in a light-controlled environment with a 12:12 hour light-dark cycle and given free access to standard mice chow and water. All animal procedures were approved by the Institutional Animal Care and Use Committee at the University of Texas Health Science Center at San Antonio and the University of Mississippi Medical Center in accordance with the "Guide for the Care and Use of Laboratory Animals". The mice underwent permanent coronary artery ligation surgery, to produce MI, as described previously.[3, 11] Three sets of mice (n 5/day/set) were used (Supplemental Table S1): one set was used for glycoproteomics, a second set was used for immunoblotting, immunohistochemistry, and immunofluorescence, and a third set was used for *in vitro* stimulation of macrophages and blood neutrophils. Supplemental Figure S1 illustrates the

workflow of the study. For all procedures, samples were randomized and analyzed in a blinded manner.

Tissue samples and protein extraction

The LV infarct region was collected at 0, 1, 3, 5, and 7 days post-MI as described previously.[3, 13] Because the insoluble fraction is enriched for ECM, we used that fraction for the glycoproteomic analysis. Immunoblotting also used the insoluble fraction for confirmation of glycoproteomic findings.

Mass spectrometry

The samples were digested with trypsin at a ratio of 1:50 (w/w, enzyme:protein) at 37°C overnight with gentle shaking. Peptide concentration was determined by BCA assay. *N*-linked glycopeptides were isolated from the tryptic peptides using the solid phase extraction of glycopeptides (SPEG) method previously reported.[14, 15] The efficiency of glycopeptide capture was evaluated previously by Zhou *et al*.[16] According to two standard proteins with isotope labeling, 85% of the glycoproteins were coupled to the hydrazide resin.

Peptides were analyzed by LC-MS/MS using a Q Exactive. MS/MS spectra were searched with SEQUEST using Proteome Discoverer (version 1.4) against the mouse RefSeq database (released in Nov 2014) containing 57,788 sequences. The False Discovery Rate was set at 0.01 to eliminate low-probability protein identifications. To eliminate false positive identifications of *N*-glycopeptides, we determined the extent of spontaneous deamidation on Asn residues satisfying the N-X-S/T sequence by profiling the unconjugated fraction of hydrazide beads without PNGase F treatment.[17, 18] The rate of spontaneous deamidation in the consensus motif was 1.5% in our sample set. Glycosylation was confirmed for several proteins, including fibronectin, γ-sarcoglycan, and periostin (Supplemental Figure S2). Peptides were quantified by label-free relative quantification based on integrated peptide peak intensities using the SIEVE software, version 2.1. Unsupervised clustering was performed using normalized peak areas of the identified glycopeptides.

Proteomic data repository

The mass spectrometry proteomics data was deposited in the ProteomeXchange Consortium (http://proteomecentral.proteomexchange.org) via the PRIDE partner repository (http://www.ebi.ac.uk/pride/) with the dataset identifier PXD001393.[19]

Bioinformatics analysis

For Gene Ontology (GO) analysis, proteins were classified to GO categories according to their cellular component and main biological processes using DAVID Bioinformatics tools (v6.7) with default settings.[20, 21] For network interaction analysis, the list of proteins was submitted to several protein-protein interaction (PPI) databases, including Database of Interacting Proteins, Molecular INTeraction database, and the Search Tool for the Retrieval of Interacting Genes/Proteins (STRING) database v9.1.[22, 23] STRING identified the most proteins from our list, therefore it was used in this study to identify protein-protein interactions using database, literature, and experimental search parameters.[23] The

confidence score was set as high (0.7). The interaction network was visualized by Cytoscape.[24]

Immunoblot analysis

Immunoblotting was used to validate proteomic findings. The insoluble fraction from the infarct area of WT or MMP-9 null mice (n=8/group; 4 male and 4 female) were analyzed. Samples were pooled for time course analysis and analyzed individually for the day 7 post-MI analysis. The blots were examined using the IQ-TL image analysis software on luminescent image analyzer. The signal intensity of each sample was normalized to the densitometry value for the total protein of its corresponding lane.

RT-PCR analysis

RNA extraction was performed on the LVI tissue as previously described.[25–27] CILP, CD36, Ltbp2, Col6a6, Col6a1, Lama5, and Fbln1 gene expression was assessed.

In vitro cleavage assay

Mouse CD36 recombinant protein was incubated with active MMP-2, MMP-9, or MMP-12 recombinant protein at a ratio of 2:1. Two negative controls (MMP alone or recombinant protein alone) were included. Samples were run on SDS-PAGE, followed by silver staining.

Immunofluorescence or immunohistochemistry

Five random images were captured at 40x magnification for analysis. Quantification was measured by Image-Pro Plus version 6.2. Representative images are shown at 40x or 60x magnification.

Phagocytosis Assay

Macrophages were isolated from day 7 post-MI LV of male mice, as previously described and stimulated with 1 ng/uL of active MMP-9, a CD36 blocking peptide (CD36i), or a combination of both (1:1 ratio).[26, 28] Phagocytosis was measured using the Vybrant Phagocytosis Kit (Life Technologies), with quantification measured on the SpectraMax M3 Plate Reader (excitation: 480 nm; emission: 520 nm). Representative images are shown at 40X magnification.

Blood neutrophil isolation and stimulation

Neutrophils were isolated from the blood of male mice as previously described.[27, 29] Cells were stimulated with 0.5 ng/uL of active MMP-9 or CD36i and harvested for RNA isolation and RT-PCR examination.

Statistical analysis

All analyses were performed blinded to groups, and data are presented as mean ± standard error of the mean (SEM). For two group comparisons, the nonparametric Wilcoxon rank sum test was used. For multiple group comparisons, the nonparametric Kruskal-Wallis test with Dunns post-test was used. A 2-way ANOVA was used for CD36 time course analysis. A value of r>0.30 was considered a strong correlation for the linear regression of CD36 and

end diastolic dimension. A p value of <0.05 was considered statistically significant. Statistical analysis was performed using GraphPad InStat3 and Prism 5.

Results

Glycoproteomic analysis identified 45 MMP-9 dependent extracellular protein changes post-MI

A total of 1161 unique *N*-linked glycopeptides were quantified by LC-MS with a 1% false discovery rate and these sites represented 541 unique glycoproteins (Supplemental Table S2). Unsupervised clustering was used to analyze the identified glycopeptides. Based on the peptide abundance, 7 of 8 WT samples and 7 of 8 MMP-9 null were clustered together, indicating good grouping based on genotype (Figure 1A). There was very poor clustering of males and females, indicating a lack of sex related differences.

A total of 122 proteins showed significant changes in MMP-9 null mice compared to WT mice (p<0.05; Supplemental Table S3). Combining a minimum two-fold change (fold change 2 or 0.5) and significance (p<0.05), there were 45 proteins (Table 1). Notably, 6 of the 45 proteins (fibronectin, collagen alpha-1, carboxypeptidase N subunit 2, beta-1 integrin, fibulin-2, and thrombospondin 1) had more than one glycopeptide identified with similar fold change, which increased the confidence for these proteins. Detailed information and quantification values can be found in Supplemental Table S2 and Supplemental Table S4. For the 20 single glycopeptides identified only once, the annotated MS/MS spectra are provided in Supplemental Figure S3. RT-PCR analysis was performed for 7 of the top 12 proteins (Supplemental Figure S4). Of note, none of the genes measured were significantly different between WT and MMP-9 null, indicating the glycoproteomic changes were not due to changes in transcription. This comparison between gene and protein levels highlights the importance of examining protein level changes in addition to gene level changes.

STRING analysis revealed that MMP-9 dependent changes work in concert as a network

To obtain an overview of the interconnections among the differentially expressed proteins, the protein list was submitted to the STRING protein-protein interaction (PPI) database and filtered for interactions of high confidence (score >0.7).[23] In Figure 1B, the up-regulated proteins are shown in red, the down-regulated proteins are shown in blue, and proteins associated with the changed proteins but not identified in this study are shown in gray. Stronger associations are represented by thick black lines, whereas weaker associations are indicated by thin gray lines. MMP-9 is highlighted in green. The analysis revealed 20 of the 45 proteins (45%) had established interconnections. For example, platelet glycoprotein 4 (CD36) is connected with thrombospondin-1 (Thbs1), and the interaction between CD36 and Thbs1 stimulates pro-apoptotic signals.[30, 31] In addition, several proteins co-regulated a common protein. For example, Tnc, Thbs1, Fn1, CD36 and Cdh2 directly or indirectly surround MMP-9 indicating these proteins act as a network.

CILP and CD36 had the highest fold increases in MMP-9 null mice

Glycoproteomics results identified cartilage intermediate layer protein (CILP) and CD36 as having the highest fold increase in MMP-9 null mice (Table 1). Since direct associations

with MMP-9 had not been previously assigned, CD36 and CILP were selected for validation (highlighted in yellow in Figure 1B). Immunoblotting was performed on an independent set of mouse tissues and showed agreement with the proteomic results (Figure 2).

Since ECM remodeling post-MI is time and space dependent, we also investigated the protein expression of CILP and CD36 in the LV infarct (LVI) or remote control (LVC) regions over the post-MI time course.[2] CILP continuously increased post-MI in both WT and MMP-9 null mice (Supplemental Figure S5). This pattern is not what we would expect if CILP was a substrate of MMP-9. For this reason, further analysis of CILP was not performed in this study. CD36 was robustly expressed at day 0, consistent with past reports of endothelial expression.[32] CD36 showed a pattern consistent with being an MMP-9 substrate; namely, it decreased over time in the WT LVI, and this decrease was attenuated by MMP-9 deletion. Surprisingly, a similar pattern was found in the remote LVC (Figure 3A). The fact that CD36 decreased in the remote region indicates additional MMPs may also cleave CD36.

MMP-9 regulates CD36 levels through proteolytic degradation

To assess *in vitro* proteolytic degradation, CD36 recombinant protein was incubated with active MMP-9. Because we found CD36 decreased over time in the remote region, we also incubated CD36 with active MMP-2 or MMP-12- two MMPs that increase in the remote region post-MI (Figure 3B). Fragments were visible with MMP-9 and MMP-12 incubation but not with MMP-2 incubation (Figure 3C and 3D). This demonstrates CD36 is cleaved by MMP-9 and MMP-12 *in vitro*, which may explain the decrease in CD36 levels observed in both the LVC and LVI samples. Interestingly, there were multiple bands generated with MMP-9 at molecular weights ranging from 50 to 10 kDa, illustrating MMP-9 not only generated a CD36 fragment but can further degrade it whereas MMP-12 only generated one major fragment. To confirm whether CD36 was cleaved by MMP-9 *in vivo*, immunoblotting was performed on the soluble fraction of homogenized LV tissue of WT and MMP-9 null mice. The results showed a 35 kDa fragment detected only in WT mice and not MMP-9 null, confirming CD36 is an *in vivo* substrate of MMP-9 (Figure 3E).

MMP-9 decreases macrophage phagocytosis

CD36 is known to be expressed by multiple cell sources, including macrophages and endothelial cells.[32, 33] At day 7 post-MI, dual immunofluorescence revealed no significant difference in the number of macrophages present in the LVI in WT and MMP-9 null mice as previously shown.[34] CD36 was significantly higher in MMP-9 null mice, consistent with glycoproteomic analysis. In addition, CD36 was co-localized with the macrophage marker Mac-3 (Figure 4). MMP-9 null mice showed higher levels of CD36+ macrophages compared to the WT mice at day 7 post-MI consistent with CD36 being reduced in WT.

CD36 expression is required for macrophage mediated phagocytosis, thus we proposed MMP-9 cleavage of CD36 would decrease phagocytosis in WT mice.[33] Macrophages isolated from the infarct of MMP-9 null mice exhibited a higher phagocytic index compared to WT macrophages (Figure 5). Stimulation with MMP-9 at concentrations similar to what is observed physiologically reduced phagocytosis by 30% in WT and 50% in MMP-9 null

indicating MMP-9 regulates phagocytosis. MMP-9 null mice had higher levels of CD36+ macrophages which explains the greater reduction in phagocytic index. To test if this decrease was due to CD36 degradation, macrophages were incubated with CD36 blocking peptide (CD36i) or a mixture of MMP-9 and CD36i. Phagocytic potential decreased to a similar extent after incubation with CD36i or the mixture indicating MMP-9 regulates phagocytosis through CD36.

MMP-9 decreased apoptotic neutrophils in infarct region at day 7 post-MI

CD36 is required for the induction of macrophage-mediated phagocytosis of apoptotic neutrophils.[35] If not removed in a timely manner, apoptotic neutrophils can continue to release granule components prolonging the inflammatory response.[36] We showed MMP-9 can degrade CD36 post-MI leading to a decrease in phagocytosis but whether this leads to sustained neutrophil inflammation is unknown. To address this, the LVs of WT and MMP-9 null mice at day 7 post-MI were stained for neutrophils. MMP-9 null had lower neutrophils numbers in the infarct region compared to WT at day 7 post-MI (Figure 6A, C). In addition to facilitating the removal of apoptotic cells, CD36 also initiates the rapid activation of caspase-3 resulting in neutrophil apoptosis.[33, 35] MMP-9 null mice had higher levels of caspase-3 and TUNEL staining compared to WT mice at day 7 post-MI (Figure 6B, D). Caspase-3–mediated spontaneous death in neutrophils is critical for modulating inflammatory responses.[37, 38] To confirm the higher levels of cleaved caspase-3 were due to neutrophil apoptosis, dual immunofluorescence of PMNs and TUNEL was performed (Figure 6E). Overlay analysis showed higher numbers of apoptotic neutrophils with MMP-9 deletion. During active inflammation, neutrophil apoptosis is delayed leading to increased tissue damage.[39]

We hypothesized that a lack of CD36 degradation was the cause of increased apoptotic neutrophils observed in the MMP-9 null mice and tested this using an *in vitro* assay. Because neutrophils are known to undergo spontaneous apoptosis in the absence of extracellular stimuli,[40–43] we used this natural process to induce apoptosis to limit exogenous influences. Incubating neutrophils with MMP-9 decreased the gene expression of the apoptotic marker caspase-9 by 2-fold and increased caspase-3, with no effect on Bax or Xiap (Figure 7). The increase in caspase-3 may be a compensatory response to the decrease in caspase-9. Caspase-9 is a critical upstream activator of the caspase pathway, and these results indicate that MMP-9 regulates apoptosis *in vitro*. CD36i increased caspase-3 and Xiap expression but did not affect caspase-9 or Bax. Xiap is an inhibitor of the caspase pathway. Our data indicates that while MMP-9 directly regulated neutrophil apoptosis, this effect was independent of CD36 degradation.

MMP-9 degradation of CD36 increases LV dilation post-MI

Excessive inflammation post-MI has been shown to impair infarct healing contributing to LV dysfunction.[7, 8, 26] At day 7 post-MI, WT mice showed increased LV dilation (Table 2), indicated by elevated diastolic dimensions and volumes compared to baseline day 0 controls. This increase was attenuated in the absence of MMP-9, consistent with previous findings.[11] Regression analysis showed decreased CD36 levels were linked to increases in end diastolic

dimensions (R^2=0.48; $p < 0.05$). MMP-9 deletion removed the link between CD36 and LV dilation.

Discussion

The goal of this study was to identify MMP-9 dependent signaling mechanisms in the post-MI LV. Our results showed that of 541 *N*-glycosylated proteins quantified, 45 proteins were at least two-fold up- or down-regulated with MMP-9 deletion; and CILP and CD36 were identified as having the highest fold increases in MMP-9 null mice. MMP-9 regulated CD36 levels through proteolytic degradation, decreasing macrophage phagocytosis and prolonging neutrophil inflammation. In addition, regression analysis showed decreased CD36 levels were linked to increases in end diastolic dimensions. Combined, our results reveal a role for MMP-9 in regulating CD36-mediated aspects of post-MI LV remodeling.

The proteins identified in this study are potential downstream mediators of MMP-9. Of the 45 differentially expressed proteins, at least five are known MMP-9 substrates, including fibronectin, collagen XIV, tenascin, laminin α5, and laminin β2.[10] Future studies identifying the role of the other key proteins identified, such as CILP and latent TGF-beta binding protein (LTBP)-2, will be necessary to fully delineate MMP-9 post-MI mechanisms. This study validated CD36 as a novel *in vivo* MMP-9 substrate. CD36 degradation delayed inflammation resolution by decreasing macrophage mediated phagocytosis. Based on our *in vitro* results, MMP-9 also regulates neutrophil apoptosis through a pathway that is not dependent on CD36 degradation.

In addition to MMP-9, CD36 was also cleaved by MMP-12. Inhibition of MMP-12 post-MI is known to suppress neutrophil apoptosis leading to prolonged inflammation and worsened LV function.[27] Interestingly, the *in vitro* cleavage assay showed multiple bands generated with MMP-9 whereas MMP-12 only generated one major fragment. This suggests that while MMP-12 cleaves CD36, MMP-9 degrades it further preventing CD36 biological activity. While MMP-9 increases only in the infarct area, MMP-12 increases in both the remote and infarct area. This is one explanation for why we see such a dramatic decrease in CD36 in the LVC. Lower levels of CD36 in the LVC could reduce fatty acid supply to the surviving myocytes, leading to a reduction in energy supply and contributing to infarct expansion.[44]

MMP-9 increases dramatically during the first week post-MI, and this lead to CD36 degradation. We focused our evaluation on day 7 post-MI, because this is a time when the early peak in MMP-9 concentrations is waning, as is the inflammatory process.[45] This time point, therefore, allows us to monitor the end points of the inflammatory process and the beginning of the scar formation process. Our study identified macrophages as a source of CD36 in the infarct. CD36 is a multifunctional plasma membrane protein that plays a role in fatty acid transport, cell apoptosis, and inflammation.[46] CD36 binds Thbs1 initiating apoptosis and the release of additional Thbs1 as a signal to recruit macrophages. The CD36/Thbs1 complex on the cell surface of the apoptotic cell acts as a ligand, which interacts with the CD36/αvβ3 complex on macrophages initiating phagocytosis of the apoptotic cell. Macrophage CD36 recognition and internalization of apoptotic cells inhibits the release of proinflammatory cytokines like tumor necrosis factor-α (TNF-α), interleukin (IL)-12, IL-1β,

and IL-8 and initiates the anti-inflammatory response which is mediated by the release of IL-10 and transforming growth factor (TGF)β.[33, 47] In our study, we showed CD36 levels decreased post-MI in WT only. This decrease was due to MMP-9 mediated degradation. Degradation of CD36 led to decreased macrophage phagocytosis at day 7 post-MI implicating MMP-9 as a key player in the persistence of the inflammatory response by mediating neutrophil removal.

Future directions

MMP-9 deletion has been proven to be beneficial post-MI in mice. However, the use of a non-specific inhibitor in clinical trials has shown to be inconclusive.[48] Our study revealed that MMP-9 plays a vital role post-MI by delaying resolution of the inflammatory response after MI. MMPs are involved in multiple biological processes, including cell-surface-receptor cleavage and release, cytokine and chemokine activation and inactivation, and ECM turnover. Understanding the entire composite of MMP-9 roles will be important for translating these findings to the clinic. Identifying the effects of MMP-9 cleavage products may provide answers and serve as novel and more selective treatment strategies for post-MI patients. Future studies utilizing full-length CD36 as well as MMP-9 derived cleavage products to rescue the phenotype are warranted. In addition, future studies utilizing CD36 null mice to investigate CD36 degradation and cardiac remodeling would further evaluate the mechanism behind this connection.

In this study, we did not evaluate the effect of CD36 degradation on metabolism or energy components. CD36 also delivers fatty acids to the myocardium for physiological energy requirements. In response to MI, the LV utilizes more energy from glucose than fatty acids leaning towards a failing phenotype.[46] MMP-9-mediated degradation of CD36 in the infarct area of the WT may reduce the fatty acid supply to the post-MI LV in WT, in contrast MMP-9 null LV showed higher levels of CD36 meeting the energy demands of the post-MI LV.[46] Future studies with a major focus on post-MI metabolic measurements and different substrate inputs will advance the field.

Conclusion

In summary, this study identified CD36 as an *in vivo* MMP-9 substrate. In the clinical setting, heart failure is marked by the persistent presence and activation of neutrophils due to their reduced clearance.[49] Our study demonstrated that degradation of CD36 decreased macrophage phagocytosis and prolonged neutrophil inflammation leading to an enlarged LV post-MI (Figure 8). These results are the first to implicate MMP-generated decreased levels of CD36 as a possible marker for sustained inflammation and heart failure.

Supplementary Material

Refer to Web version on PubMed Central for supplementary material.

Acknowledgments

References

1. Roger VL, Go AS, Lloyd-Jones DM, Benjamin EJ, Berry JD, Borden WB, et al. Heart disease and stroke statistics--2012 update: A report from the american heart association. Circulation. 2012; 125:e2–e220. [PubMed: 22179539]

2. Jourdan-Lesaux C, Zhang J, Lindsey ML. Extracellular matrix roles during cardiac repair. Life Sci. 2010; 87:391–400. [PubMed: 20670633]

3. Zamilpa R, Zhang J, Chiao YA, de Castro Bras LE, Halade GV, Ma Y, et al. Cardiac wound healing post-myocardial infarction: A novel method to target extracellular matrix remodeling in the left ventricle. Methods Mol Biol. 2013; 1037:313–324. [PubMed: 24029944]

4. Lindsey ML. Mmp induction and inhibition in myocardial infarction. Heart Fail Rev. 2004; 9:7–19. [PubMed: 14739764]

5. Van Lint P, Libert C. Chemokine and cytokine processing by matrix metalloproteinases and its effect on leukocyte migration and inflammation. J Leukoc Biol. 2007; 82:1375–1381. [PubMed: 17709402]

6. Ducharme A, Frantz S, Aikawa M, Rabkin E, Lindsey M, Rohde LE, et al. Targeted deletion of matrix metalloproteinase-9 attenuates left ventricular enlargement and collagen accumulation after experimental myocardial infarction. J Clin Invest. 2000; 106:55–62. [PubMed: 10880048]

7. Tao ZY, Cavasin MA, Yang F, Liu YH, Yang XP. Temporal changes in matrix metalloproteinase expression and inflammatory response associated with cardiac rupture after myocardial infarction in mice. Life Sci. 2004; 74:1561–1572. [PubMed: 14729404]

8. Heymans S, Luttun A, Nuyens D, Theilmeier G, Creemers E, Moons L, et al. Inhibition of plasminogen activators or matrix metalloproteinases prevents cardiac rupture but impairs therapeutic angiogenesis and causes cardiac failure. Nat Med. 1999; 5:1135–1142. [PubMed: 10502816]

9. Zamilpa R, Lopez EF, Chiao YA, Dai Q, Escobar GP, Hakala K, et al. Proteomic analysis identifies in vivo candidate matrix metalloproteinase-9 substrates in the left ventricle post-myocardial infarction. Proteomics. 2010; 10:2214–2223. [PubMed: 20354994]

10. Zitka O, Kukacka J, Krizkova S, Huska D, Adam V, Masarik M, et al. Matrix metalloproteinases. Curr Med Chem. 2010; 17:3751–3768. [PubMed: 20846107]

11. Lindsey ML, Escobar GP, Dobrucki LW, Goshorn DK, Bouges S, Mingoia JT, et al. Matrix metalloproteinase-9 gene deletion facilitates angiogenesis after myocardial infarction. Am J Physiol Heart Circ Physiol. 2006; 290:H232–239. [PubMed: 16126817]

12. Vu TH, Shipley JM, Bergers G, Berger JE, Helms JA, Hanahan D, et al. Mmp-9/gelatinase b is a key regulator of growth plate angiogenesis and apoptosis of hypertrophic chondrocytes. Cell. 1998; 93:411–422. [PubMed: 9590175]

13. de Castro Bras LE, Ramirez TA, DeLeon-Pennell KY, Chiao YA, Ma Y, Dai Q, et al. Texas 3-step decellularization protocol: Looking at the cardiac extracellular matrix. J Proteomics. 2013; 86:43–52. [PubMed: 23681174]

14. Zhang H, Li XJ, Martin DB, Aebersold R. Identification and quantification of n-linked glycoproteins using hydrazide chemistry, stable isotope labeling and mass spectrometry. Nat Biotechnol. 2003; 21:660–666. [PubMed: 12754519]

15. Tian Y, Zhou Y, Elliott S, Aebersold R, Zhang H. Solid-phase extraction of n-linked glycopeptides. Nat Protoc. 2007; 2:334–339. [PubMed: 17406594]

16. Zhou Y, Aebersold R, Zhang H. Isolation of n-linked glycopeptides from plasma. Anal Chem. 2007; 79:5826–5837. [PubMed: 17591751]

17. Palmisano G, Melo-Braga MN, Engholm-Keller K, Parker BL, Larsen MR. Chemical deamidation: A common pitfall in large-scale n-linked glycoproteomic mass spectrometry-based analyses. J Proteome Res. 2012; 11:1949–1957. [PubMed: 22256963]

18. Wright HT. Nonenzymatic deamidation of asparaginyl and glutaminyl residues in proteins. Crit Rev Biochem Mol Biol. 1991; 26:1–52. [PubMed: 1678690]

19. Vizcaino JA, Deutsch EW, Wang R, Csordas A, Reisinger F, Rios D, et al. Proteomexchange provides globally coordinated proteomics data submission and dissemination. Nat Biotechnol. 2014; 32:223–226. [PubMed: 24727771]

20. Huang da W, Sherman BT, Lempicki RA. Systematic and integrative analysis of large gene lists using david bioinformatics resources. Nat Protoc. 2009; 4:44–57. [PubMed: 19131956]

21. Huang da W, Sherman BT, Lempicki RA. Bioinformatics enrichment tools: Paths toward the comprehensive functional analysis of large gene lists. Nucleic Acids Res. 2009; 37:1–13. [PubMed: 19033363]

22. Salwinski L, Miller CS, Smith AJ, Pettit FK, Bowie JU, Eisenberg D. The database of interacting proteins: 2004 update. Nucleic Acids Res. 2004; 32:D449–451. [PubMed: 14681454]

23. Jensen LJ, Kuhn M, Stark M, Chaffron S, Creevey C, Muller J, et al. String 8--a global view on proteins and their functional interactions in 630 organisms. Nucleic Acids Res. 2009; 37:D412–416. [PubMed: 18940858]

24. Shannon P, Markiel A, Ozier O, Baliga NS, Wang JT, Ramage D, et al. Cytoscape: A software environment for integrated models of biomolecular interaction networks. Genome Res. 2003; 13:2498–2504. [PubMed: 14597658]

25. Deleon-Pennell KY, Bras LE, Lindsey ML. Circulating lipopolysaccharide resets cardiac homeostasis in mice through a matrix metalloproteinase-9 dependent mechanism. Physiol Rep. 2013; 1:e00079. [PubMed: 24159380]

26. DeLeon-Pennell KY, de Castro Bras LE, Iyer RP, Bratton DR, Jin YF, Ripplinger CM, et al. P. Gingivalis lipopolysaccharide intensifies inflammation post-myocardial infarction through matrix metalloproteinase-9. J Mol Cell Cardiol. 2014; 76C:218–226. [PubMed: 25240641]

27. Iyer RP, Patterson NL, Zouein FA, Ma Y, Dive V, de Castro Bras LE, et al. Early matrix metalloproteinase-12 inhibition worsens post-myocardial infarction cardiac dysfunction by delaying inflammation resolution. Int J Cardiol. 2015; 185:198–208. [PubMed: 25797678]

28. Zamilpa R, Kanakia R, Cigarroa Jt, Dai Q, Escobar GP, Martinez H, et al. Cc chemokine receptor 5 deletion impairs macrophage activation and induces adverse remodeling following myocardial infarction. Am J Physiol Heart Circ Physiol. 2011; 300:H1418–H1426. [PubMed: 21297029]

29. Oh H, Siano B, Diamond S. Neutrophil isolation protocol. J Vis Exp. 2008; 17:745. [PubMed: 19066523]

30. Qin L, Kim E, Ratan R, Lee FS, Cho S. Genetic variant of bdnf (val66met) polymorphism attenuates stroke-induced angiogenic responses by enhancing anti-angiogenic mediator cd36 expression. J Neurosci. 2011; 31:775–783. [PubMed: 21228186]

31. Seftor RE, Seftor EA, Stetler-Stevenson WG, Hendrix MJ. The 72 kda type iv collagenase is modulated via differential expression of alpha v beta 3 and alpha 5 beta 1 integrins during human melanoma cell invasion. Cancer Res. 1993; 53:3411–3415. [PubMed: 7686818]

32. Swerlick RA, Lee KH, Wick TM, Lawley TJ. Human dermal microvascular endothelial but not human umbilical vein endothelial cells express cd36 in vivo and in vitro. J Immunol. 1992; 148:78–83. [PubMed: 1370173]

33. Fadok VA, Warner ML, Bratton DL, Henson PM. Cd36 is required for phagocytosis of apoptotic cells by human macrophages that use either a phosphatidylserine receptor or the vitronectin receptor (alpha v beta 3). J Immunol. 1998; 161:6250–6257. [PubMed: 9834113]

34. Lindsey ML, Escobar GP, Dobrucki LW, Goshorn DK, Bouges S, Mingoia JT, et al. Matrix metalloproteinase-9 gene deletion facilitates angiogenesis after myocardial infarction. Am J Physiol Heart Circ Physiol. 2006; 290:H232–H239. [PubMed: 16126817]

35. Ma Y, Yabluchanskiy A, Lindsey ML. Neutrophil roles in left ventricular remodeling following myocardial infarction. Fibrogenesis Tissue Repair. 2013; 6:11. [PubMed: 23731794]

36. Bratton DL, Henson PM. Neutrophil clearance: When the party is over, clean-up begins. Trends Immunol. 2011; 32:350–357. [PubMed: 21782511]

37. Loison F, Zhu H, Karatepe K, Kasorn A, Liu P, Ye K, et al. Proteinase 3-dependent caspase-3 cleavage modulates neutrophil death and inflammation. J Clin Invest. 2014; 124:4445–4458. [PubMed: 25180606]

38. Savill J, Hogg N, Ren Y, Haslett C. Thrombospondin cooperates with cd36 and the vitronectin receptor in macrophage recognition of neutrophils undergoing apoptosis. J Clin Invest. 1992; 90:1513–1522. [PubMed: 1383273]

39. Cheah FC, Hampton MB, Darlow BA, Winterbourn CC, Vissers MC. Detection of apoptosis by caspase-3 activation in tracheal aspirate neutrophils from premature infants: Relationship with nf-kappab activation. J Leukoc Biol. 2005; 77:432–437. [PubMed: 15604122]

40. Kirschnek S, Vier J, Gautam S, Frankenberg T, Rangelova S, Eitz-Ferrer P, et al. Molecular analysis of neutrophil spontaneous apoptosis reveals a strong role for the pro-apoptotic bh3-only protein noxa. Cell Death Differ. 2011; 18:1805–1814. [PubMed: 21660046]

41. Frumento G, Ottonello L, Bertolotto M, Franchello S, Melioli G, Dallegri F. Spontaneous apoptosis in neutrophils is associated with downregulation of hla class i and is prevented by ligation of class i. J Leukoc Biol. 2000; 68:873–880. [PubMed: 11129655]

42. Savill JS, Wyllie AH, Henson JE, Walport MJ, Henson PM, Haslett C. Macrophage phagocytosis of aging neutrophils in inflammation. Programmed cell death in the neutrophil leads to its recognition by macrophages. J Clin Invest. 1989; 83:865–875. [PubMed: 2921324]

43. Akgul C, Moulding DA, Edwards SW. Molecular control of neutrophil apoptosis. FEBS Lett. 2001; 487:318–322. [PubMed: 11163351]

44. Irie H, Krukenkamp IB, Brinkmann JF, Gaudette GR, Saltman AE, Jou W, et al. Myocardial recovery from ischemia is impaired in cd36-null mice and restored by myocyte cd36 expression or medium-chain fatty acids. Proc Natl Acad Sci U S A. 2003; 100:6819–6824. [PubMed: 12746501]

45. Patterson NL, Iyer RP, de Castro Bras LE, Li Y, Andrews TG, Aune GJ, et al. Using proteomics to uncover extracellular matrix interactions during cardiac remodeling. Proteomics Clin Appl. 2013; 7:516–527. [PubMed: 23532927]

46. Bonen A, Tandon NN, Glatz JF, Luiken JJ, Heigenhauser GJ. The fatty acid transporter fat/cd36 is upregulated in subcutaneous and visceral adipose tissues in human obesity and type 2 diabetes. Int J Obes (Lond). 2006; 30:877–883. [PubMed: 16418758]

47. Fadok VA, Bratton DL, Konowal A, Freed PW, Westcott JY, Henson PM. Macrophages that have ingested apoptotic cells in vitro inhibit proinflammatory cytokine production through autocrine/paracrine mechanisms involving tgf-beta, pge2, and paf. J Clin Invest. 1998; 101:890–898. [PubMed: 9466984]

48. Hudson MP, Armstrong PW, Ruzyllo W, Brum J, Cusmano L, Krzeski P, et al. Effects of selective matrix metalloproteinase inhibitor (pg-116800) to prevent ventricular remodeling after myocardial infarction: Results of the premier (prevention of myocardial infarction early remodeling) trial. J Am Coll Cardiol. 2006; 48:15–20. [PubMed: 16814643]

49. Benites-Zapata VA, Hernandez AV, Nagarajan V, Cauthen CA, Starling RC, Tang WH. Usefulness of neutrophil-to-lymphocyte ratio in risk stratification of patients with advanced heart failure. Am J Cardiol. 2015; 115:57–61. [PubMed: 25456873]

Clinical Perspective

In the United States, >40% of all deaths are attributed to cardiovascular disease (CVD), and more than half of these deaths are due to myocardial infarction (MI). Following MI, the cardiac extracellular matrix (ECM) is proteolytically cleaved by matrix metalloproteinases (MMPs). MMPs are involved in multiple biological processes, including cell-surface-receptor cleavage and release, cytokine and chemokine activation and inactivation, and ECM turnover. MMP-9 deletion has been shown to be beneficial post-MI in mice, however, the use of non-specific MMP inhibitors have been inconclusive in clinical trials. The current article used a proteomic strategy to identify novel MMP-9 substrates. Platelet glycoprotein 4, CD36, was validated as a novel *in vivo* MMP-9 substrate. Degradation of CD36 by MMP-9 decreased macrophage phagocytosis and prolonged neutrophil inflammation. This study revealed that MMP-9 deletion promotes resolution of the inflammatory response. Identifying the effects of MMP-9 cleavage products may provide novel therapeutic insight for post-MI patients.
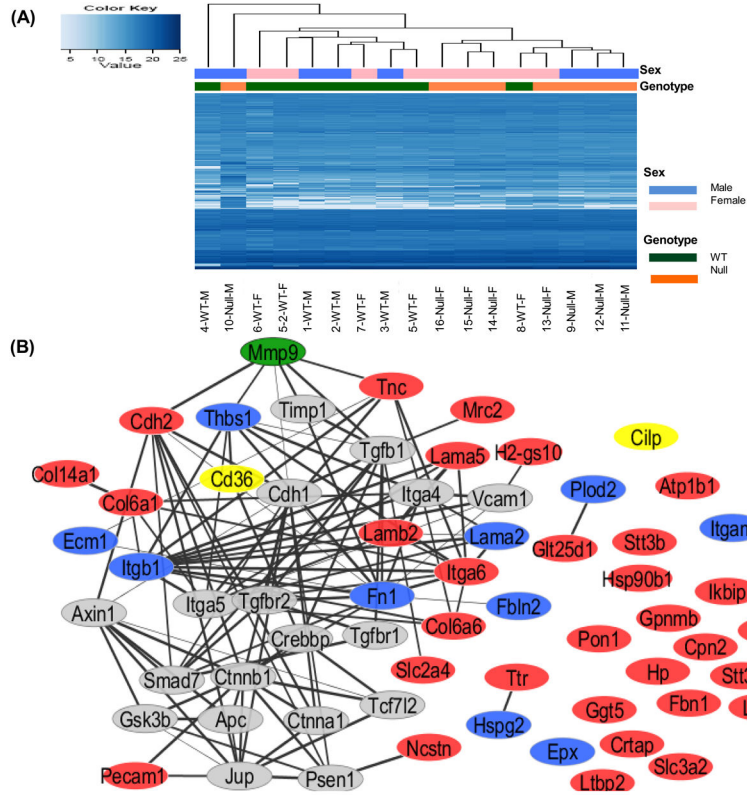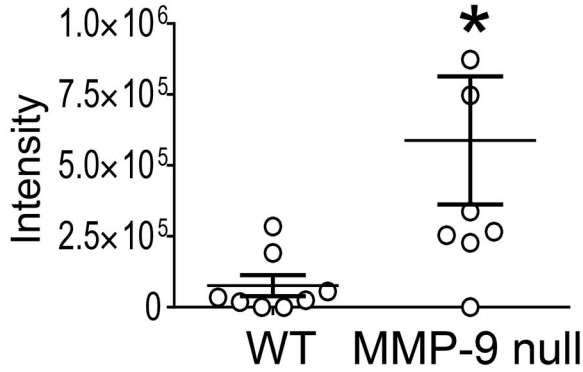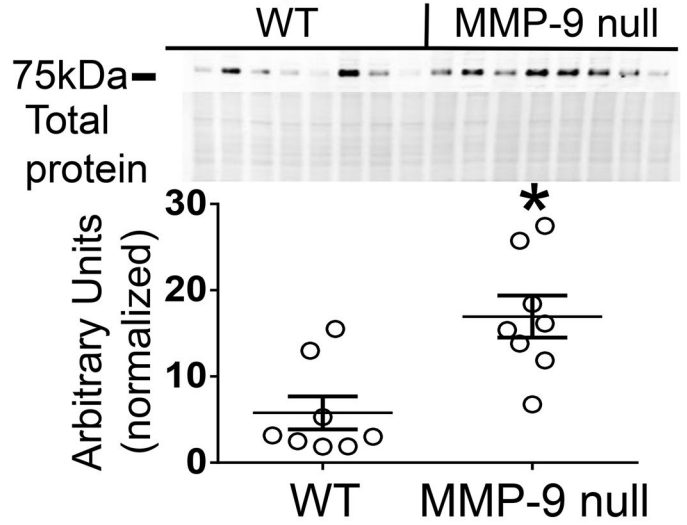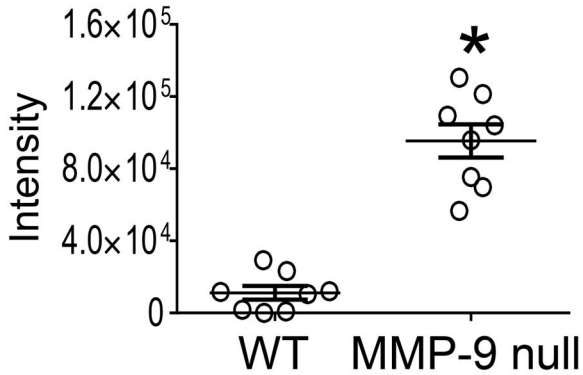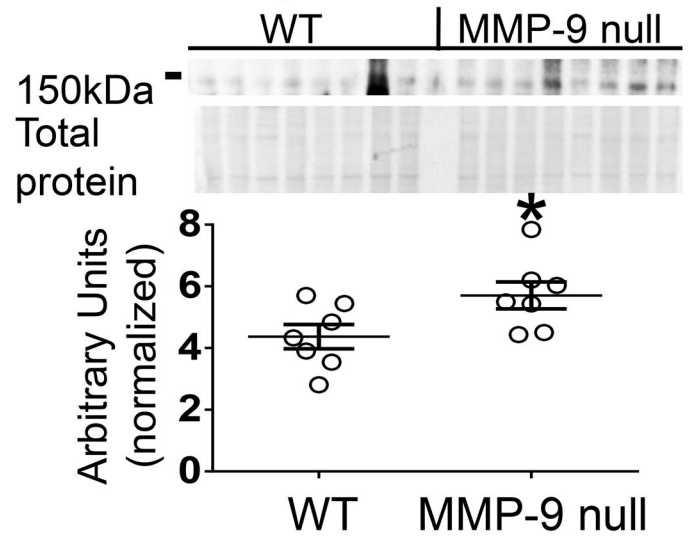
Figure 1.
Glycoproteomic analysis identified MMP-9 dependent extracellular protein changes post-myocardial infarction (MI). (**A**) Unsupervised clustering of the identified glycopeptides was performed using normalized peak areas. WT samples and MMP-9 null clustered separately, with the exception of one WT and one null sample. Sex differences were not observed. (**B**) The changed proteins were analyzed by STRING (Search Tool for the Retrieval of Interacting Genes/Proteins v9.1) protein-protein interaction (PPI) software with high confidence (score >0.7) and visualized by Cytoscape. The majority of the changed proteins interacted with each other. Stronger associations are represented by thicker lines. Red nodes are the up-regulated proteins, blue nodes are the down-regulated proteins, and gray nodes present proteins associated with the changed proteins. MMP-9 is highlighted in green. CD36 and CILP, highlighted in yellow, were selected for immunoblot analysis.

Figure 2.

MMP-9 deletion increased CD36 and CILP levels at day 7 post-myocardial infarction (MI). Immunoblotting analysis of the LV infarct (LVI) at day 7 post MI using individual mice. (**A**) CD36 and (**B**) CILP increased in MMP-9 null mice, which is consistent with the proteomic results (left panel). Data are represented as mean ± SEM. *p < 0.05 vs WT; n=8/group.
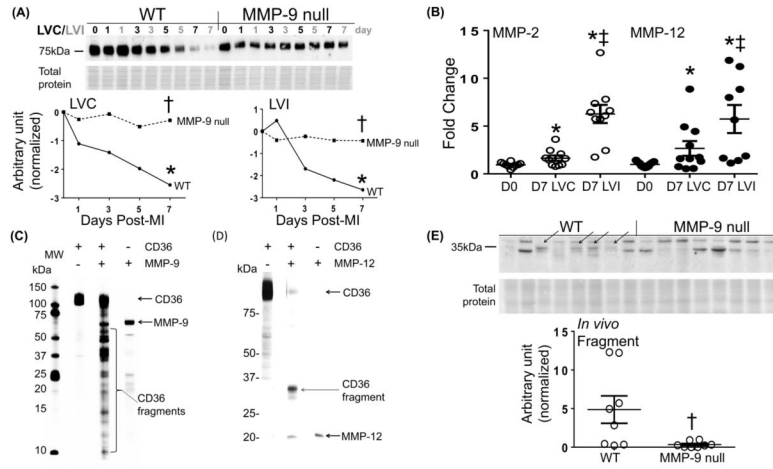
Figure 3.
MMP-9 regulates CD36 levels through proteolytic degradation. (**A**) Full length CD36 decreased over time in the LV infarct (LVI) of WT mice post-myocardial infarction (MI) and this decrease was attenuated by MMP-9 deletion. A similar pattern was found in the remote control (LVC). (**B**) MMP-2 and -12 increased in both the LVC and LVI at day 7 post-MI compared to day 0. *In vitro* cleavage assay showed recombinant CD36 was cleaved by active (**C**) MMP-9 and (**D**) MMP-12. Silver staining showed CD36 fragments as indicated by bracket. (**E**) Immunoblotting of the soluble fraction of homogenized LV tissue of WT and MMP-9 null mice using CD36 antibody showed a 35 kDa fragment detected largely in WT mice but not MMP-9 null, confirming CD36 is an *in vivo* substrate of MMP-9. Data are represented as mean ± SEM. *$p < 0.05$ vs respective D0; †$p < 0.05$ vs WT; ‡$p < 0.05$ vs D7 LVC; n=8/group.
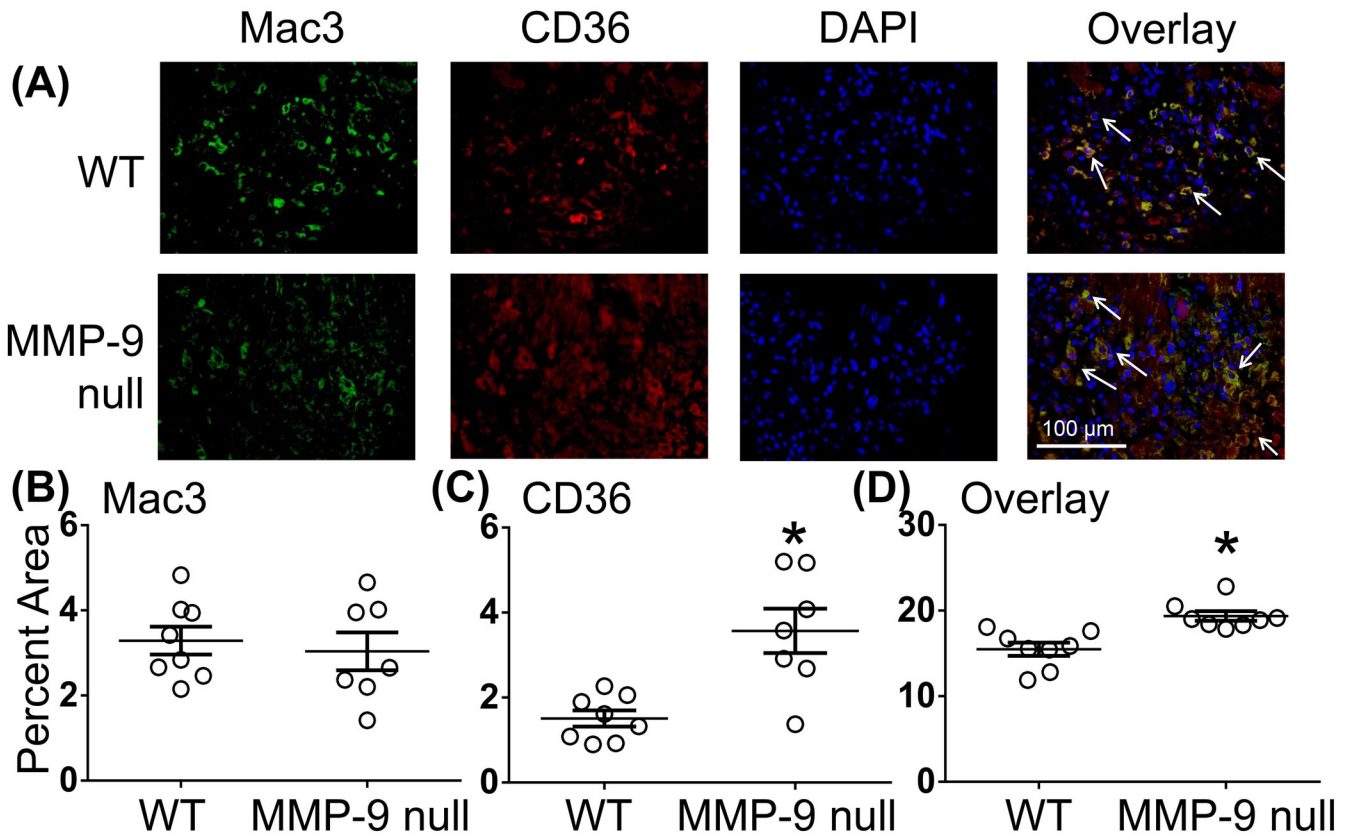
Figure 4.
MMP-9 regulates macrophage expression of CD36. (**A**) Representative dual immunofluorescence images. (**B**) WT and MMP-9 null animals had similar numbers of Mac3 positive cells in the infarct at day 7 post-myocardial infarction (MI). (**C**) CD36 expression was increased in MMP-9 null animals similar to what was observed by proteomics and immunoblotting analysis. (**D**) Overlay analysis indicated CD36 was largely expressed by macrophages. Staining showed higher levels of CD36+ macrophages in the MMP-9 null mice at day 7 post-MI. Data are represented as mean ± SEM. *p< 0.05 vs WT; n=8/group.
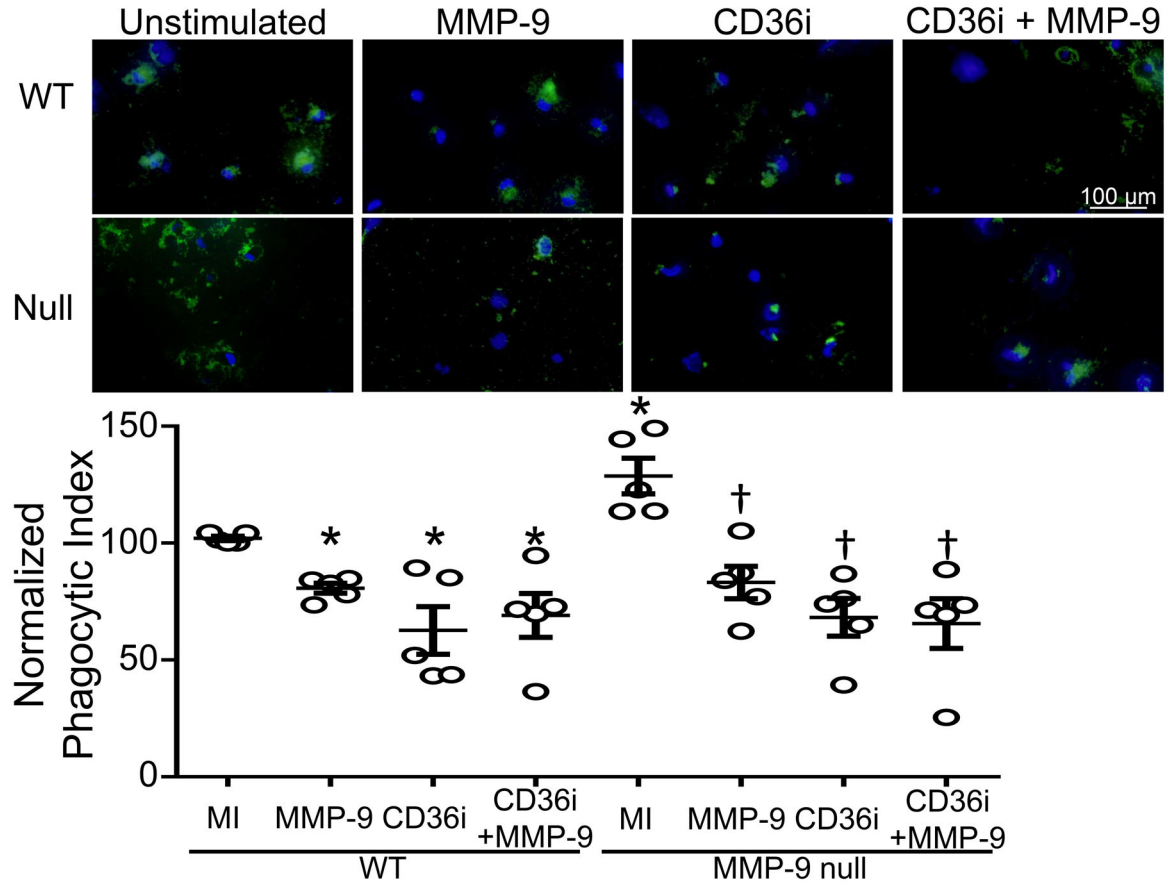
Figure 5.
MMP-9 regulates phagocytosis through CD36. As shown by the *in vivo* stimulated cells isolated from day 7 post-myocardial infarction left ventricle (MI), MMP-9 deletion increases macrophage phagocytic index compared to WT macrophages. MMP-9 incubation decreased phagocytosis in both WT and MMP-9 null. MMP-9, CD36 blocking peptide (CD36i) and the combination of MMP-9 and CD36i decreased phagocytosis to similar degrees, indicating MMP-9 regulates macrophage phagocytic potential through CD36. Quantification of phagocytosis was performed using the SpectraMax M3 Plate Reader. Data are represented as mean ± SEM. Representative images are at 40X magnification. Fluorescent Bioparticles are shown in green. DAPI staining is shown in blue. *p< 0.05 vs WT; †p< 0.05 vs vs null MI; n=5/group.
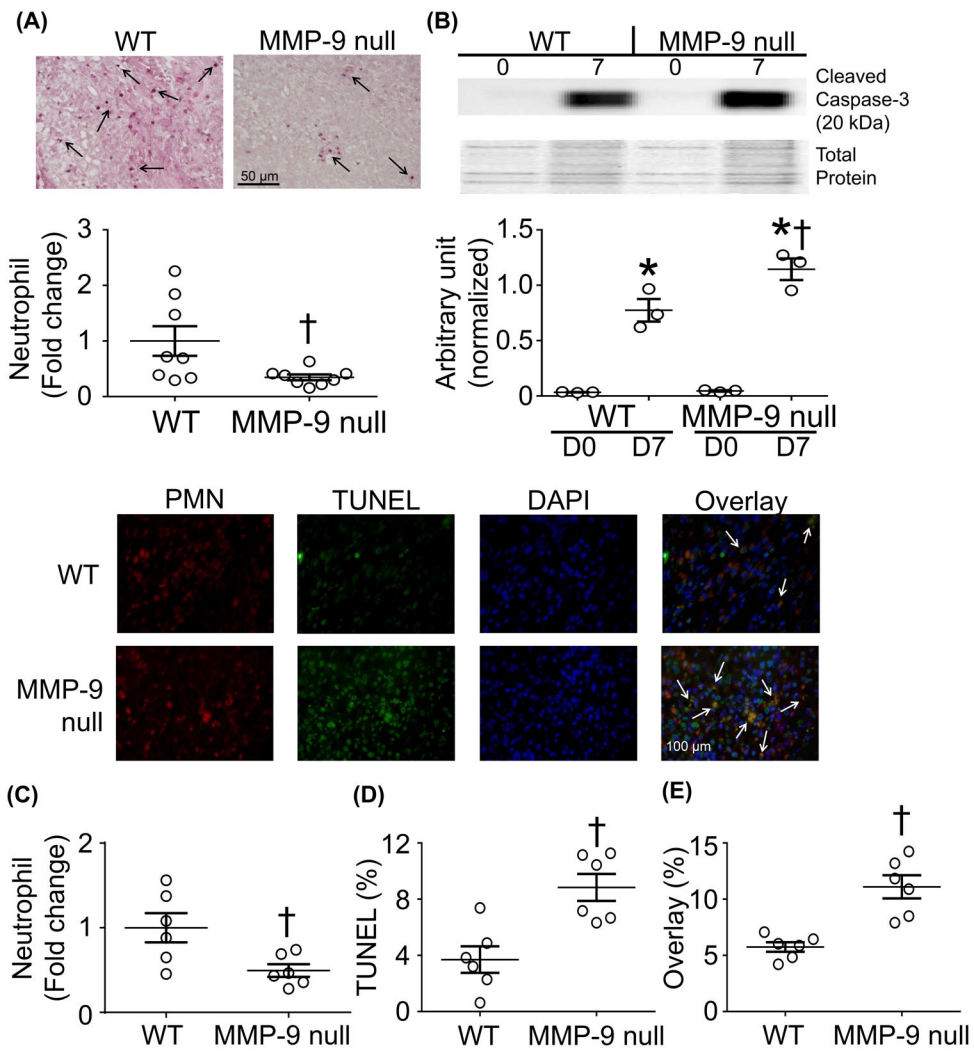
Figure 6.
MMP-9 decreases removal of apoptotic neutrophils post-myocardial infarction (MI). (**A, C**) MMP-9 null mice had lower numbers of neutrophils in the infarct at day 7 post-MI compared to WT. This decrease was coupled with an increase in the apoptotic markers (**B**) cleaved caspase-3 (pooled samples) and (**D**) terminal deoxynucleotidyl transferase dUTP nick end labeling (TUNEL) at day 7 post-MI. (**E**) Overlay analysis indicated lower numbers of apoptotic neutrophils in WT animals indicating prolonged neutrophil mediated inflammation at day 7 post-MI. Data are represented as mean ± SEM. *p< 0.05 vs respective D0; †p< 0.05 vs WT; n=8/group.
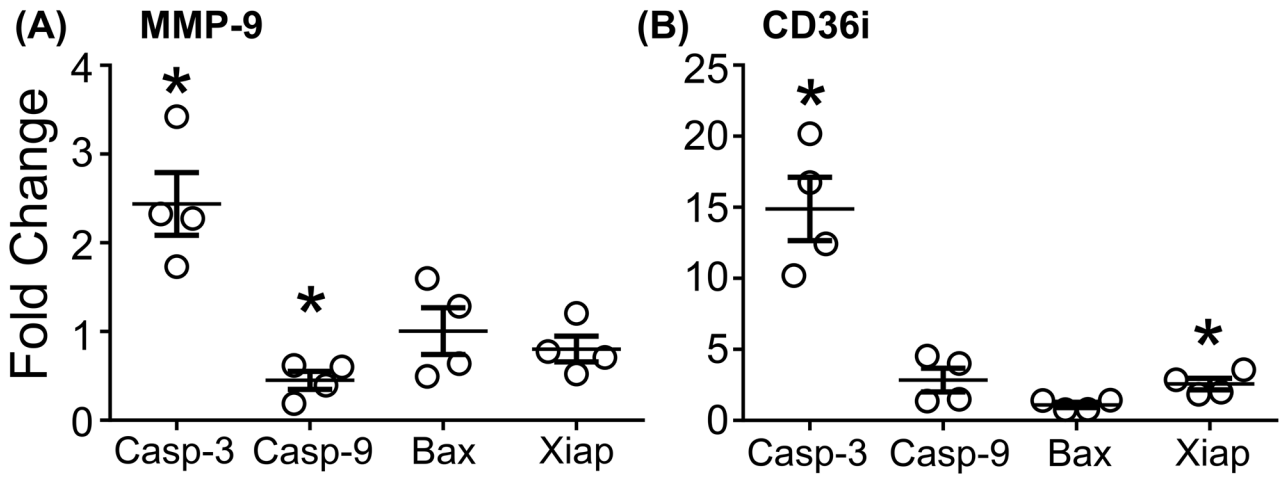
Figure 7.
MMP-9 inhibits apoptosis in blood neutrophils. (**A**) Compared to unstimulated cells MMP-9 decreased neutrophil expression of caspase-9 and increased caspase-3 expression but had no effect on Bax or Xiap. (**B**) CD36 blocking peptide (CD36i) increased expression of capsase-3 in addition to the apoptotic inhibitor, Xiap, indicating that while MMP-9 does regulate apoptosis, it is not through CD36 degradation. Stimulated data was normalized to unstimulated data to illustrate fold change. Data are represented as mean ± SEM. *p< 0.05 vs unstimulated; n=4/group.

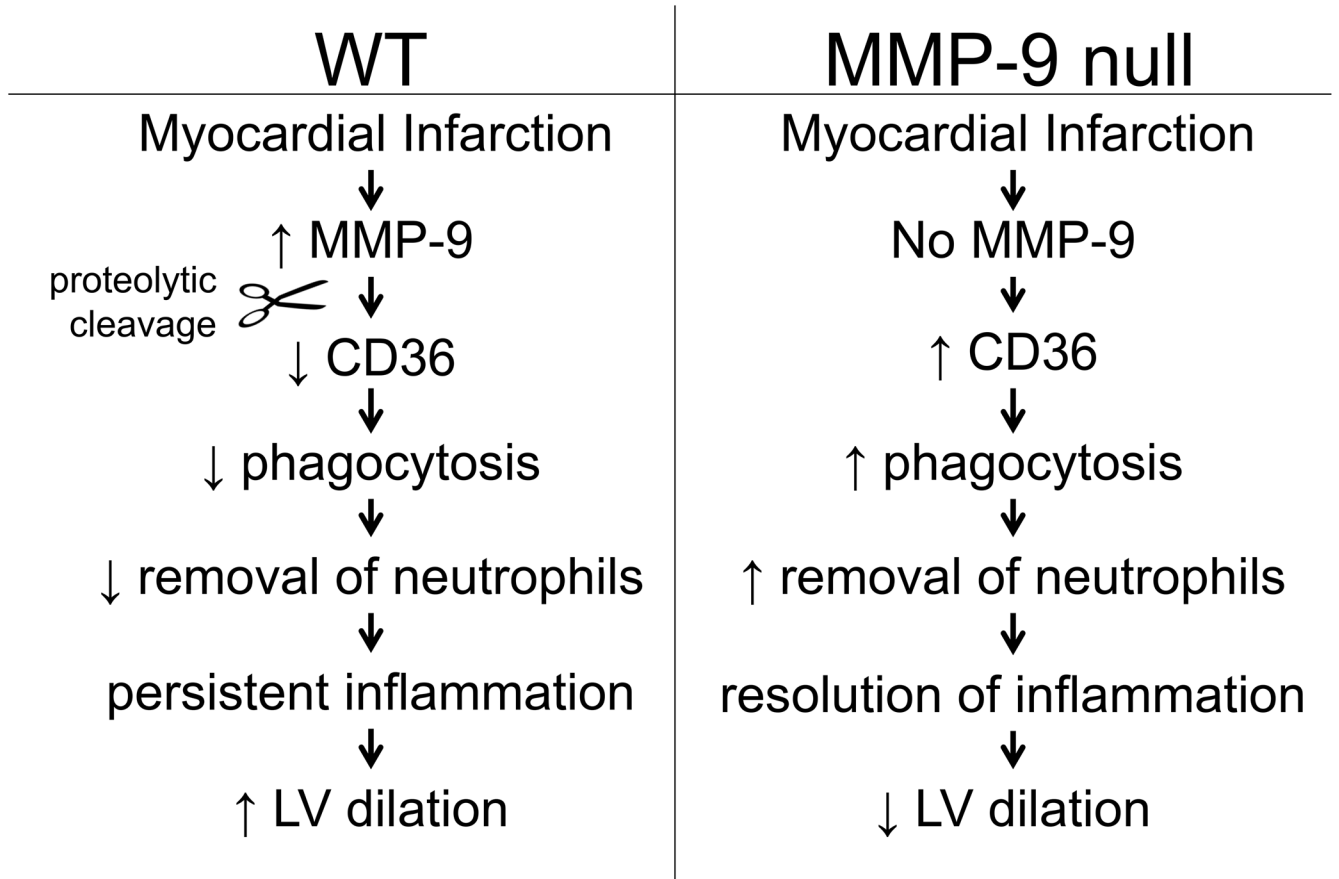| WT	MMP-9 null
Myocardial Infarction	Myocardial Infarction
↓	↓
↑ MMP-9	No MMP-9
proteolytic cleavage ✂ ↓	↓
↓ CD36	↑ CD36
↓	↓
↓ phagocytosis	↑ phagocytosis
↓	↓
↓ removal of neutrophils	↑ removal of neutrophils
↓	↓
persistent inflammation	resolution of inflammation
↓	↓
↑ LV dilation	↓ LV dilation

Figure 8.
Diagram depicting the roles of MMP-9 mediated CD36 degradation in LV remodeling post-myocardial infarction (MI). Following MI, MMP-9 degradation of CD36 resulted in decreased phagocytic index and prolonged neutrophil inflammation, leading to LV dysfunction.

Table 1

Proteins differentially expressed in MMP-9 null mice (all p < 0.05 and at least two-fold difference), ordered by normalized ratio (NR; null/WT; normalized to total ion current by SIEVE) to evaluate substrate accumulation in the absence of MMP-9.

Accession number	Protein Description	Cellular component	Glycopeptides	NR	N-p Value
27734196	Cartilage intermediate layer protein (CILP)	Extracellular matrix	EQRPGQNCSNYTVR	13.13	9.90E-07
56893000	Platelet glycoprotein 4 (CD36)	Plasma membrane	QFWIFDVQNPDDVAK NSSK	9.35	2.90E-02
158341636	Latent-transforming growth factor beta-binding protein 2	Extracellular region	DSSPQAAHVNHLSPPWGLNLTEK	7.12	1.60E-02
6753138	Sodium/potassium-transporting ATPase subunit beta-1	Plasma membrane	LDWLGNCSGLNDDSYGYR	6.74	8.60E-03
156616286	Collagen alpha-6 (VI)	Extracellular matrix	LNANLLSSLWDTFQNK	6.37	4.00E-02
6753484	Collagen alpha-1 (VI)	Extracellular matrix	RNFTAADWGHSR	5.25	3.70E-02
568920137	Laminin subunit alpha-5	Extracellular matrix	EQLQGINASSAAWAR	5.09	4.80E-02
61651673	Dolichyl-diphosphooligosaccharide--protein glycosyltransferase subunit STT3B	Endoplasmic reticulum membrane	TTLVDNNTWNNSHIALVGK	4.81	2.70E-02
170784829	Procollagen galactosyltransferase 1	Unknown	TALWVATDHNTDNTSAILR	4.34	2.30E-02
238637279	4F2 cell-surface antigen heavy chain	Plasma membrane	APLMPWNESSIFHIPRPVSLNMTVK	4.33	2.00E-02
755498697	Fibrillin-1	Extracellular matrix	AWGTPCELCPSVNTSEYK	4.29	3.20E-02
			CDSGFALDSEERNCTDIDECR	0.45	4.50E-02
568911077	Nicastrin	Plasma membrane	ANNSWFQSILK	4.14	3.20E-02
755537649	Platelet endothelial cell adhesion molecule	Plasma membrane	EKEDRPFHQAVVNDTQAFWHNK	4.1	1.20E-02
568939471	Serum paraoxonase/arylesterase 1	Extracellular region	HANWTLTPLK	4.05	3.80E-02
568926396	Tenascin	Extracellular matrix	ASTEEVPSLENLTVTEAGWDGLR	3.89	2.50E-02
31982236	Integrin alpha 6	Plasma membrane	LWNSTFLEEYSK	3.76	5.00E-03
			SFMVNWTQSPGK	3.75	3.70E-02
568991244	Collagen alpha-1 (XIV)	Extracellular matrix	VVDKGNGSKPTSPEEVK	2.18	3.60E-02
171846253	Transmembrane glycoprotein NMB	Unknown	NLSDEIFLR	3.66	3.20E-02
124494256	Prolow-density lipoprotein receptor-related protein 1	Plasma membrane	WTGHNVTVVQR	3.62	2.40E-02
148747128	Dolichyl-diphosphooligosaccharide--protein glycosyltransferase subunit STT3A	Membrane	TILVDNNTWNNTHISR	3.52	2.20E-02
6755863	Endoplasmin	Plasma membrane	HNNDTQHIWESDSNEFSVIADPR	3.36	3.60E-02
121674797	Palmitoyl-protein thioesterase	Golgi apparatus	FFNDSIVDPVDSEWFGFYR	3.29	4.40E-02
225543173	Cartilage-associated protein	Extracellular matrix	DKWGLSDEHFQPRPEAVQFFNVTTLQK	3.05	3.20E-02
569003077	Cadherin-2	Plasma membrane	RNWTINR	3.03	1.00E-02

Circ Cardiovasc Genet. Author manuscript; available in PMC 2017 February 01.

Accession number	Protein Description	Cellular component	Glycopeptides	NR	N-p Value
755537859	Solute carrier family 2, facilitated glucose transporter member 4	Plasma membrane	VIEQSYNATWLGR	2.71	8.70E-03
31542891	Gamma-glutamyltransferase 5	Plasma membrane	LWDPSSHPGIQNISR	2.65	2.50E-02
121583481	Inhibitor of nuclear factor kappa-B kinase-interacting protein, isoform 1	Endoplasmic reticulum membrane	FQNITDFWK	2.52	4.70E-02
8850219	Haptoglobin	Extracellular region	VVLHPNHSVVDIGLIK	2.36	1.00E-02
568972029	C-type mannose receptor 2	Cell surface	ASNASKPGTLER	2.18	3.80E-02
568962784	Laminin subunit beta-2	Extracellular matrix	AQAALDKANASR	2.14	2.10E-02
7305599	Transthyretin	Extracellular region	TLGISPFHEFADVVFTANDSGHR	2.08	1.70E-02
147904569	Carboxypeptidase N subunit 2	Extracellular region	LQDLEITGSPVSNLSAHIFSNLSSLEK	2.08	4.80E-02
			LSLDSNNLTALHPALFHNLSR	2.02	2.50E-03
31982712	Carboxypeptidase B2	Extracellular region	IPFNVLMNNVEDLIEQQTFNDTVSPR	2.07	2.50E-02
219521935	MHC class I like protein GS10	Plasma membrane	TLLSYYNQSAGGSHTIQVISGCEVGSDGR	2.02	2.70E-03
45504394	Integrin beta-1	Plasma membrane	KDTCAQECSHFNLTK	0.5	3.70E-02
			KENSSEICSNNGECVCGQCVCR	0.37	2.90E-02
755522163	Integrin alpha-M	Plasma membrane	TPVLNCSVAVCK	0.49	5.20E-03
			WTPLNSSTIIGYR	3.65	4.10E-02
449083336	Fibronectin	Extracellular matrix	VFAVHQGRESNPLTAQQTTKLDAPTNLQFVNETDR	0.5	1.60E-02
			HEEGHMLNCTCFGQGR	0.43	2.50E-02
			RHEEGHMLNCTCFGQGR	0.35	2.10E-02
			SNDSVLEPANR	0.49	4.60E-02
269315863	Collagen alpha-5 (VI)	Unknown	LEGVTMFAMGIEGANNTQLEDIVSYPSR	0.44	4.20E-02
			SSANQSEFQQQIQK	0.38	8.60E-03
166064058	Slit homolog 2 protein	Unknown	DLEVLTLNNNNITR	0.48	8.90E-03
218931165	Procollagen-lysine,2-oxoglutarate 5-dioxygenase 2	Endoplasmic reticulum membrane	YNCSIESPR	0.47	1.50E-02
568940646	Fibulin-2	Extracellular matrix	EGETCGAEDNDTCGVSLYK	0.46	4.30E-03
			DLDECALGTHNCSEAETCHNIQGSFR	0.37	1.40E-02
568930638	Basement membrane-specific heparan sulfate proteoglycan core protein	Extracellular matrix	CDGDFDCEDRTDEANCSVK	0.44	4.60E-02
47059073	Thrombospondin 1	Extracellular region	GCSSSATNVLLTLDNNVVNGSSPAIR	0.39	2.30E-02
			VSCPIMPCSNATVPDGECCPR	0.32	8.10E-03
145966840	Eosinophil peroxidase	Cytoplasmic granule	ALLPFDNLHEDPCLLTNR	0.28	7.50E-03

Accession number	Protein Description	Cellular component	Glycopeptides	NR	N-p Value
358030288	Extracellular matrix protein 1	Extracellular matrix	QIPGLIQNMTIR	0	8.10E-06

glycosylation motif is indicated in **bold**

N-p value: Normalized p value

Table 2

While dilation of the left ventricle occurred in both WT and MMP-9 null mice at Day 7 post-myocardial infarction (MI), MMP-9 deletion attenuated this effect.

	WT		MMP-9 null	
	Day 0 (n=8)	Day 7 (n=16)	Day 0 (n=8)	Day 7 (n=16)
Infarct size (%)	NA	53±3	NA	52±2
Heart Rate (bpm)	473±14	473±11	440±7	450±11
LV Infarct Wall Thickness (mm)	1.20±0.07	0.65±0.05*	1.13±0.03	0.68±0.05*
End Diastolic Dimension (mm)	3.47±0.10	5.79±0.18*	3.52±0.05	5.14±0.24*†
End Systolic Dimension (mm)	2.16±0.08	5.42±0.19*	2.14±0.06	4.78±0.26*
Fractional Shortening %	38±1	6±1*	39±2	7±1*
End Diastolic Volume (uL)	58±2	160±10*	54±2	124±10*†
End Systolic Volume (uL)	17±1	140±10*	15±1	107±10*
Ejection Fraction (%)	70±1	12±1*	72±1	15±2*

Day 0 are naive, no MI controls. Values are means ± SEM.

* vs p<0.05 vs respective baseline

† vs p<0.05 vs WT Day 7